

Heavy-Fermion Superconductivity in the Quadrupole Ordered State of $\text{PrV}_2\text{Al}_{20}$

Masaki Tsujimoto,¹ Yosuke Matsumoto,¹ Takahiro Tomita,¹ Akito Sakai,¹ and Satoru Nakatsuji^{1,2,*}

¹*Institute for Solid State Physics, University of Tokyo, Kashiwa, Chiba 277-8581, Japan*

²*PRESTO, Japan Science and Technology Agency (JST), 4-1-8 Honcho Kawaguchi, Saitama 332-0012, Japan*

(Received 21 June 2014; published 23 December 2014)

$\text{PrV}_2\text{Al}_{20}$ is a rare example of a heavy-fermion system based on strong hybridization between conduction electrons and nonmagnetic quadrupolar moments of the cubic Γ_3 ground doublet. Here, we report that a high-quality single crystal of $\text{PrV}_2\text{Al}_{20}$ exhibits superconductivity at $T_c = 50$ mK in the antiferroquadrupole-ordered state under ambient pressure. The heavy-fermion character of the superconductivity is evident from the specific heat jump of $\Delta C/T \sim 0.3$ J/mol K² and the effective mass $m^*/m_0 \sim 140$ estimated from the temperature dependence of the upper critical field. Furthermore, the high-quality single crystals exhibit double transitions at $T_Q = 0.75$ K and $T^* = 0.65$ K associated with quadrupole and octupole degrees of freedom of the Γ_3 doublet. In the ordered state, the specific heat C/T shows a T^3 dependence, indicating the gapless mode associated with the quadrupole order, the octupole order, or both. The strong sensitivity to impurity of the superconductivity suggests unconventional character due to significant quadrupolar fluctuations.

DOI: 10.1103/PhysRevLett.113.267001

PACS numbers: 74.70.Tx, 75.25.Dk, 72.15.Qm

$4f$ electron systems exhibit a large variety of nontrivial ground states by tuning the hybridization between localized $4f$ and conduction (c -) electrons. The emergence of exotic superconductivity (SC) with a large effective mass from unconventional quantum criticality has attracted particular attention [1–5]. While most of the examples have been reported at the border of magnetism [6,7], similarly exotic states of matter may be found in the vicinity of the quantum phase transition associated with different degrees of freedom of f electrons, such as electrical quadrupole (orbital) and valence. In particular, experimental exploration of the quadrupolar instability is important since few studies on the associated quantum criticality have been made to date.

For the exploration, the simplest example could be found in materials that carry no magnetic but quadrupole moments. Such a nonmagnetic ground state is known as the Γ_3 doublet in the cubic crystalline electric field (CEF) of an f^2 configuration. Intensive studies have revealed various interesting states in the cubic Γ_3 doublet systems, in particular in Pr-based intermetallic compounds [8–12]. However, Pr-based cubic Γ_3 doublet systems usually have well-localized quadrupole moments, and thus until quite recently there have been no studies on the quadrupolar instability by tuning the c - f hybridization.

$\text{PrTr}_2\text{Al}_{20}$ (Tr = Ti, V) has been reported as a rare example of cubic Γ_3 doublet-based Kondo lattice systems where one may tune the hybridization strength between quadrupole moments and conduction electrons by chemical substitution and by pressure [13,14]. These materials have the nonmagnetic Γ_3 CEF ground state with the well-separated excited state at $\Delta_{\text{CEF}} \sim 60$ K (Ti) and 40 K (V), as confirmed by various experiments [13,15,16], and exhibit the respective ferro- and antiferroquadrupole

ordering at $T_Q = 2.0$ K (Ti) and 0.6 K (V) [13,15,17]. Significantly, strong c - f hybridization is evident from a number of phenomena, including the Kondo effect in the resistivity, the Kondo resonance peak observed near the Fermi energy, and the large hyperfine constant in NMR measurements [13,18,19]. In addition, the hybridization can be enhanced by chemical substitution. In fact, $\text{PrV}_2\text{Al}_{20}$ exhibits chemical pressure effects such as the enhanced Kondo effect, a large Weiss temperature, and the suppression of the quadrupolar ordering, compared to the Ti analog. Besides, in contrast with the localized properties of $\text{PrTi}_2\text{Al}_{20}$, $\text{PrV}_2\text{Al}_{20}$ exhibits non-Fermi liquid behavior above T_Q [13], which may be attributed to the quadrupolar Kondo effects [20].

The recent discovery of heavy-fermion superconductivity in the vicinity of the putative quadrupolar quantum critical point (QCP) has clearly demonstrated the tunable strong hybridization in $\text{PrTi}_2\text{Al}_{20}$ [14,21]. At ambient pressure, $\text{PrTi}_2\text{Al}_{20}$ shows superconductivity at $T_c = 0.2$ K in the ferroquadrupole ordered state [21]. Effective mass estimated from the upper critical field is moderately enhanced with $m^*/m_0 \sim 16$. Application of pressure significantly increases T_c and m^* up to $T_c \sim 1$ K and $m^*/m_0 \sim 110$ at ~ 8 GPa while suppressing T_Q , indicating the emergence of the heavy-fermion SC in the vicinity of the QCP of the quadrupolar order [14].

In this Letter, we report the first observation of heavy-fermion SC in a cubic Γ_3 doublet compound under ambient pressure. In particular, we discover the superconductivity in an antiferroquadrupolar state of $\text{PrV}_2\text{Al}_{20}$ below $T_c = 0.05$ K in a high-quality single crystal. Both the field dependence of the upper critical field and the specific heat measurements indicate the enhanced effective mass as

high as $m^*/m_0 \sim 140$ and the specific heat coefficient $\gamma \sim 0.9$ J/mol K². Our study using high-quality single crystals also reveals the double transition associated with the Γ_3 doublet, suggesting that not only quadrupolar but octupolar degrees play important roles.

The success in growing high-quality single crystals has allowed us to observe the superconductivity in PrV₂Al₂₀. The details of the experimental method are in the Supplemental Material [22]. Figure 1(a) shows the temperature dependence of the resistivity $\rho(T)$ for one of the highest quality crystals with residual resistivity ratio (RRR) ~ 19 . For comparison, we also plot $\rho(T)$ for PrTi₂Al₂₀. Clearly, PrV₂Al₂₀ exhibits a resistivity drop due to the SC transition at $T_c = 0.05$ K, as indicated by an arrow. The SC transition was also found in another sample (RRR ~ 18) at a slightly lower $T_c = 0.039$ K, as displayed in Fig. 1(b). We further checked the sample with RRR ~ 4 and 7 and did not find any sign of SC, at least down to 38 and 43 mK, respectively. Our results suggest that T_c strongly depends

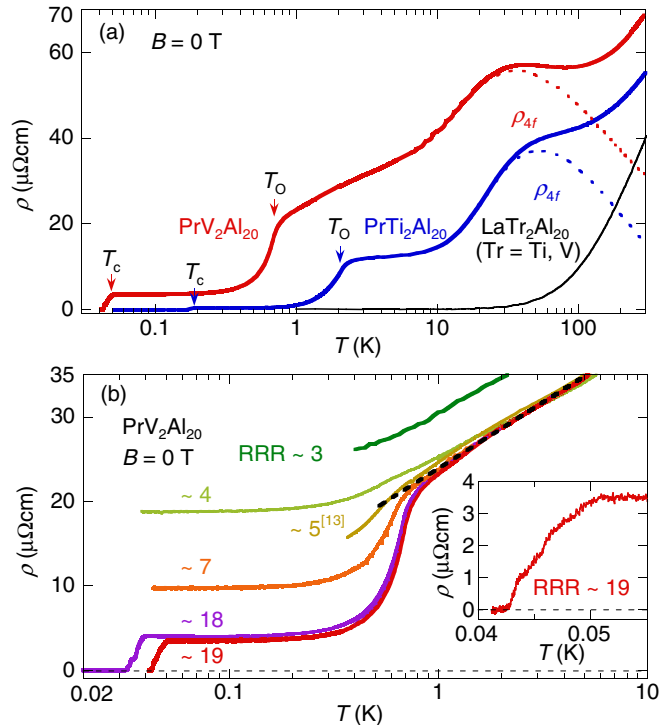


FIG. 1 (color online). (a) Temperature dependence of the resistivity $\rho(T)$ for the single crystals of PrV₂Al₂₀ (RRR ~ 19) and PrTi₂Al₂₀ (RRR ~ 150) under the Earth's field. $4f$ electron contribution ρ_{4f} is calculated by subtracting the T dependence of the inelastic part of ρ for LaTr₂Al₂₀ indicated by the solid line. Arrows indicate the peak temperatures found in $d\rho/dT$, $T_0 = 0.68$ K (V) and 2.0 K (Ti), and the superconducting transitions at $T_c = 0.05$ K (V) and 0.2 K (Ti), respectively. (b) $\rho(T)$ of PrV₂Al₂₀ below 10 K for various crystals with different qualities, including the crystal with RRR ~ 19 in panel (a). The $\rho(T)$ of the crystal with RRR ~ 18 was scaled for $\rho(T)$ with RRR ~ 19 at $1 \text{ K} < T < 10 \text{ K}$. A fit to a $\ln T$ curve is shown as a broken line at $T > T_0$. Inset: $\rho(T)$ of the crystal with RRR ~ 19 at around T_c .

on RRR, suggesting an unconventional character of the SC. Further measurements are necessary to clarify their detailed relation. The other arrows in Fig. 1(a) indicate the peak temperatures T_0 found in the $d\rho/dT$ associated with quadrupolar ordering. A single peak in $d\rho/dT$ at $T_0 = 0.68$ K higher than the previous report [13] was observed for the crystal with RRR ~ 19 , while clear double transitions at $T_0 = 0.75$ K and $T^* = 0.65$ K were found in the specific heat measurements using almost the same quality crystal (RRR ~ 20) that we will discuss. The dotted lines indicate the $4f$ -electron contribution to the resistivity ρ_{4f} , calculated by subtracting off the inelastic part of the resistivity of LaTr₂Al₂₀ (Tr = Ti, V) shown by the solid line. $\rho_{4f} \propto -\ln T$ observed above $T_{\text{peak}} \sim 60$ K (Ti) and ~ 40 K (V) should be the magnetic Kondo effect, as the magnetic excited CEF states are populated at $T > T_{\text{peak}} \sim \Delta_{\text{CEF}}$ [13].

To verify the bulk superconductivity, we measured the dc and ac susceptibility of a high-quality crystal (RRR ~ 20). Figure 2(a) shows the T dependence of the dc susceptibility $\chi(T)$ of PrV₂Al₂₀ under a field of $\mu_0 H = 0.1$ mT along the [110] direction. The volume fraction was estimated to be 82% (ZFC) and 47% (FC), indicating the bulk SC. The large diamagnetic signal comparable to the Al shielding signal is also observed in the T dependence of the real part of the ac susceptibility $\chi'(T)$ under zero dc field and ac field ~ 0.1 μ T (Fig. 2 inset).

To clarify the boundary of the SC phase, we measured the susceptibility and resistivity under various fields. As a summary, Fig. 3 shows the T dependence of the upper critical field B_{c2} for PrV₂Al₂₀. For comparison, we show the results for PrTi₂Al₂₀ as well [21]. Here, the critical temperatures (the diamonds) are determined by the onset of the anomaly of the susceptibility, as defined by the foot of the peak shown by arrows in the Fig. 3 inset. Compared to PrTi₂Al₂₀, the peak in the susceptibility around T_c due to the

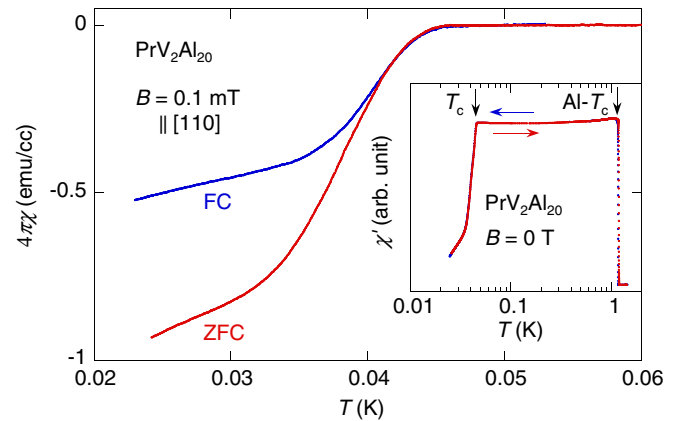


FIG. 2 (color online). Temperature dependence of the dc susceptibility $\chi(T)$ for the single crystal of PrV₂Al₂₀ (RRR ~ 20) under the field of 0.1 mT for zero field cooled (ZFC) and field cooled (FC) sequences. (Inset) The real part of the ac susceptibility $\chi'(T)$ for PrV₂Al₂₀ and the reference of Al.

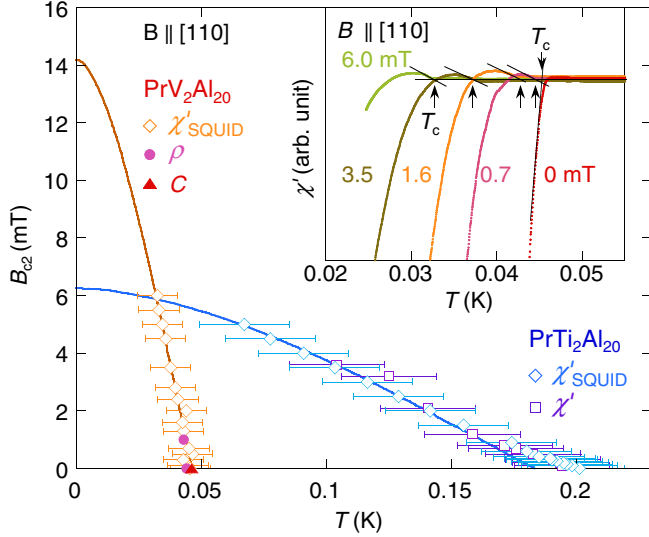


FIG. 3 (color online). T dependence of the upper critical field B_{c2} for the single crystals of $\text{PrV}_2\text{Al}_{20}$ (RRR ~ 20) and $\text{PrTi}_2\text{Al}_{20}$ (RRR ~ 150) under a field along [110]. The square, diamond, circle, and triangle data points are determined by ac susceptibility, ac susceptibility by SQUID, resistivity, and specific heat measurements, respectively. Solid lines represent the fit based on the WHH model. (Inset) T dependence of the real part of the ac susceptibility χ' for $\text{PrV}_2\text{Al}_{20}$ under various magnetic fields. Arrows indicate the critical temperatures.

differential paramagnetic effect is quite small in $\text{PrV}_2\text{Al}_{20}$ [30], indicating a strong pinning effect typical of the type II SC. The critical temperatures defined above are consistent with the zero-resistance temperature (the circles) of the SC drop of $\rho(T)$ (Fig. 3). The solid line in Fig. 3 is the fit to our B_{c2} results based on the Werthamer-Helfand-Hohenberg (WHH) model [31,32]. The best fitting was obtained using parameters of $T_c = 46.2$ mK and the slope of B_{c2} at T_c , $B'_{c2} \equiv dB_{c2}/dT = 0.41$ T/K. The model reproduces the experimental data well, indicating that the orbital depairing effect is dominant. The resultant orbital critical field at $T = 0$, $B_{c2}^{\text{orb}}(0) = -0.727B'_{c2}T_c$, and the Ginzburg-Landau (GL) coherence length, $\xi = \sqrt{\Phi_0/2\pi B_{c2}^{\text{orb}}(0)}$, are $B_{c2}^{\text{orb}}(0) = 14.3$ mT and $\xi = 0.15$ μm , respectively.

Strikingly, B'_{c2} of $\text{PrV}_2\text{Al}_{20}$ is about 10 times larger than the Ti analog [21], indicating a significantly heavier effective mass. Indeed, the effective mass is estimated to be $m^* = \hbar k_F/v_F \sim 140m_0$ by using the GL coherence length $\xi = 0.15$ μm , the Fermi velocity $v_F = \xi k_B T_c / (0.18\hbar) = 5.1$ km/s, $k_F = (3\pi^2 Z/\Omega) = 6.1 \times 10^9$ 1/m, where Z is the number of electrons per unit cell and Ω is the unit-cell volume. The effective mass $m^*/m_0 \sim 140$ is much larger than the $m^*/m_0 \sim 16$ estimated for $\text{PrTi}_2\text{Al}_{20}$ under ambient pressure [21] and is comparable to $m^*/m_0 \sim 110$ under ~ 8 GPa in the vicinity of the quadrupolar quantum criticality [14]. Thus, the mass enhancement in $\text{PrV}_2\text{Al}_{20}$ indicates not only the strong c - f hybridization, but also its proximity to a quadrupolar QCP.

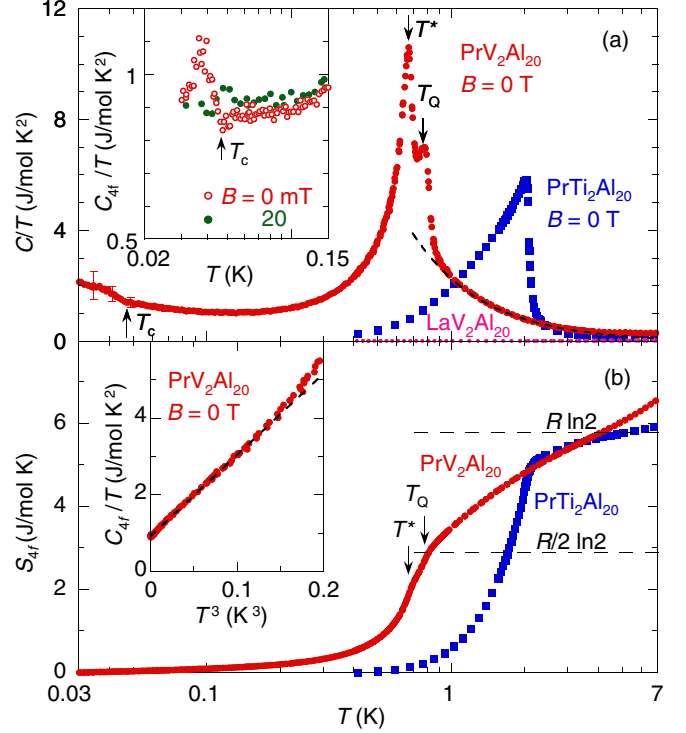


FIG. 4 (color online). (a) T dependence of the specific heat divided by T , C/T for $\text{PrV}_2\text{Al}_{20}$ and $\text{PrTi}_2\text{Al}_{20}$ under the Earth's field. Double transition temperatures T_Q and T^* are defined at the peaks. The broken line indicates the fit to $C/T \sim 1/T^{3/2}$ in the paraquadrupolar state. As for the error bars at $T < T_c$, see Ref. [22]. (Inset) T dependence of C_{4f}/T for $\text{PrV}_2\text{Al}_{20}$ under $B = 0$ (open circle), 20 mT (closed circle). C_{4f}/T was derived by subtracting the contribution of the lattice and nuclear magnetism from C/T . (b) T dependence of the entropy S_{4f} for $\text{PrV}_2\text{Al}_{20}$ and $\text{PrTi}_2\text{Al}_{20}$. The horizontal broken lines show the value of $R \ln 2$ and $R/2 \ln 2$, respectively. The inset shows C_{4f}/T vs T^3 for the T range at $T < 0.58$ K. The broken line represents the linear fit, indicating that C_{4f}/T shows T^3 dependence in 0.05 K $< T < 0.5$ K.

The heavy-fermion character of the SC was also confirmed by the specific heat (C) measurements. Figure 4(a) shows the C/T of $\text{PrV}_2\text{Al}_{20}$. In comparison, the lattice contribution estimated from the C/T of $\text{LaV}_2\text{Al}_{20}$ is found to be small and negligible. After showing a broad minimum at $T \sim 0.12$ K, the C/T slightly increases on cooling and exhibits an anomaly at $T = 0.046$ K, corresponding to the SC transition. The low T upturn in C/T becomes evident in the normal state stabilized under the magnetic field of 20 mT and is found to follow $C/T \sim 1/T^2$ down to the lowest T of 30 mK. This power law increase, $C \sim 1/T$, seen at $T < 100$ mK indicates an entropy release associated with a very small energy scale of mK range, most likely coming from a nuclear magnetism. Actually, hyperfine-enhanced nuclear magnetism is often reported for Pr intermetallic compounds with a nonmagnetic ground state. Indeed, the analysis based on the μSR measurements also indicated the hyperfine-enhanced nuclear magnetism in $\text{PrTi}_2\text{Al}_{20}$ and estimated the transition temperature of

0.13 mK [17]. In addition, the $C \sim 1/T^\alpha$ ($\alpha \sim 1$) behavior has been commonly seen in the T range close to the nuclear magnetic transition. For example, PrNi₅, a prototypical system of the hyperfine-enhanced nuclear magnetism, exhibits $C \sim 1/T^\alpha$ ($\alpha \sim 1$) behavior in the similar T range below 100 mK down near the ordering temperature of 0.4 mK [33].

Thus, we estimated the $4f$ -electron contribution of the specific heat divided by T , C_{4f}/T by subtracting the low T upturn ($\sim 1/T^2$) coming from the nuclear magnetism, as shown in the inset of Fig. 4(a). The zero field SC anomaly is evident in indicating its bulk character, which can be suppressed under the field of 20 mT. The nearly constant C_{4f}/T in the normal state provides an estimate of the large electronic coefficient $\gamma \sim 0.9$ J/mol K², consistent with the above estimate of the effective mass $m^*/m_0 \sim 140$. From the sudden increase of C_{4f}/T at T_c , one may estimate the SC jump in γ , $\Delta C/T_c \sim 0.3$ J/mol K², which provides direct evidence of the heavy-fermion SC. This yields the ratio $\Delta C/(\gamma T_c) \sim 0.3$, which is much smaller than the BCS value of 1.43. It will be an interesting future issue to determine whether the transition becomes much sharper as the sample quality is further improved.

In the normal state, we clearly observed two peaks of the specific heat at $T_Q = 0.75$ K and $T^* = 0.65$ K, indicating double transitions, as discussed by K. Araki *et al.* in Ref. [34] [Fig. 4(a)]. The double transition was not found in the sample with RRR ~ 6 [13] but was observed only in relatively high RRR (> 7) samples [34], and it was thereby an intrinsic phenomenon. Given the fact that both quadrupole and octupole degrees of freedom are available in the Γ_3 doublet state and may not necessarily coexist with each other, one interesting possibility is that the high and low temperature transitions are due to the octupole and quadrupole ordering, respectively.

Strong hybridization between quadrupole moments and conduction electrons not only is the key to understanding heavy-fermion SC but also induces various interesting effects in the normal state. A hybridization effect is seen in the temperature dependence of the entropy $S(T)$ obtained after the integration of C_{4f}/T vs T . As shown in Fig. 4(b), $S(T)$ of PrV₂Al₂₀ reaches $R \ln 2$ around 4 K $\sim 6T_Q$ and is further suppressed on cooling down to 50% of $R \ln 2$ at T_Q , while the suppression is much weaker and retains 90% at T_Q in the Ti analog. The release of the Γ_3 entropy over a wide T range below $6T_Q$ cannot be ascribed to the critical fluctuations associated with the quadrupolar ordering. Instead, it should come from the screening of quadrupole moments by conduction electrons through the strong hybridization. In the same T region, we have seen various anomalous metallic properties far different from the Fermi liquid (FL) behavior. For example, C_{4f}/T shows an unusual increase proportional to $T^{-3/2}$, as shown in Fig. 4(a), while the magnetic susceptibility exhibits $-T^{1/2}$ dependence [13]. In addition, $\rho(T)$ behaves as $\rho(T) \propto \ln T$

[Fig. 1(b)], which is far different from the FL $\rho(T) \propto T^2$ law seen in PrTi₂Al₂₀. One possible scenario for the origin of the anomalous metal is the quadrupolar Kondo effect. Interestingly, $S(T)$ becomes exactly $R/2 \ln 2$ at T_Q , as expected for the quadrupolar Kondo effect.

As indicated in Fig. 1(b), only the highest quality samples exhibit the sharp drop of the resistivity at the quadrupolar transition. The resistivity drop below T_Q gradually broadens and finally disappears for RRR < 4 . On the other hand, the $\rho(T)$ curves in the paraquadrupolar state at $T > T_Q$ overlap on top for the samples with RRR > 4 . This indicates that the inelastic process governing $\rho(T)$ does not depend on the impurity concentration and thus is local in character. It is most likely that the anomalous metallic state arises from the *local screening* of quadrupole moments of the Γ_3 state through, for example, the quadrupolar Kondo effect.

Strong hybridization also affects the excitation spectrum in the quadrupolar ordered state. Because of the anisotropic character, quadrupole moments normally form an excitation gap in the ordered state. Indeed, PrTi₂Al₂₀ displays the exponential decay of the specific heat and resistivity below T_Q [21,35]. In PrV₂Al₂₀, however, the temperature dependence of C_{4f} below T_Q shows the T^4 power law behavior. The Fig. 4(b) inset indicates that the T^3 dependence of C_{4f}/T is in the temperature range between 0.05 K and 0.5 K. This suggests a gapless mode due to the quadrupolar order in PrV₂Al₂₀, corresponding to the “orbiton” in transition metal systems [36].

In addition to the heavy mass character of the superconductivity, the anomalous metallic state in the paraquadrupolar state and the gapless quadrupolar excitations in the ordered state may well come from the competition between the quadrupole order and the screening effects due to strong hybridization and would therefore be the signatures of strong quadrupole fluctuations arising from the proximity to a quadrupolar quantum phase transition. It is highly likely that the pairing of heavy-fermion superconductivity is mediated by such fluctuations. It is thus quite interesting to study the pressure effect of a high-quality single crystal of PrV₂Al₂₀. As PrV₂Al₂₀ has stronger hybridization than PrTi₂Al₂₀, the putative quantum phase transition and the associated heavy-fermion superconductivity would emerge at a much lower pressure than in PrTi₂Al₂₀.

We thank Y. Karaki, Y. Uwatoko, K. Matsubayashi, J. Suzuki, T. Sakakibara, Y. Shimura, K. Araki, Y.-B. Kim, E. C. T. O’Farrell, K. Kuga, and K. Ueda for their support and the useful discussions. This Letter was partially supported by PRESTO of JST and Grants-in-Aid (No. 25707030) from the Japanese Society for the Promotion of Science (JSPS), by Grants-in-Aids for Scientific Research on Innovative Areas “Heavy Electrons” of the Ministry of Education, Culture, Sports, Science and Technology, Japan. The use of the facilities of

the Materials Design and Characterization Laboratory at the Institute for Solid State Physics, The University of Tokyo is gratefully acknowledged. One of the authors, (M. T.) was supported by the JSPS through Program for Leading Graduate Schools (MERIT).

*satoru@issp.u-tokyo.ac.jp

- [1] F. Steglich, J. Aarts, C. D. Bredl, W. Lieke, D. Meschede, W. Franz, and H. Schäfer, *Phys. Rev. Lett.* **43**, 1892 (1979).
- [2] N. D. Mathur, F. M. Grosche, S. R. Julian, I. R. Walker, D. M. Freye, R. K. W. Haselwimmer, and G. G. Lonzarich, *Nature (London)* **394**, 39 (1998).
- [3] H. Hegger, C. Petrovic, E. G. Moshopoulou, M. F. Hundley, J. L. Sarrao, Z. Fisk, and J. D. Thompson, *Phys. Rev. Lett.* **84**, 4986 (2000).
- [4] C. Petrovic, P. G. Pagliuso, M. F. Hundley, R. Movshovich, J. L. Sarrao, J. D. Thompson, Z. Fisk, and P. Monthoux, *J. Phys. Condens. Matter* **13**, L337 (2001).
- [5] S. Nakatsuji, K. Kuga, Y. Machida, T. Tayama, T. Sakakibara, Y. Karaki, H. Ishimoto, S. Yonezawa, Y. Maeno, E. Pearson *et al.*, *Nat. Phys.* **4**, 603 (2008).
- [6] H. V. Löhneysen, A. Rosch, M. Vojta, and P. Wölfle, *Rev. Mod. Phys.* **79**, 1015 (2007).
- [7] P. Gegenwart, Q. Si, and F. Steglich, *Nat. Phys.* **4**, 186 (2008).
- [8] P. Morin, D. Schmitt, and E. du Tremolet de Lacheisserie, *J. Magn. Magn. Mater.* **30**, 257 (1982).
- [9] H. Suzuki, M. Kasaya, T. Miyazaki, Y. Nemoto, and T. Goto, *J. Phys. Soc. Jpn.* **66**, 2566 (1997).
- [10] T. Onimaru, T. Sakakibara, N. Aso, H. Yoshizawa, H. S. Suzuki, and T. Takeuchi, *Phys. Rev. Lett.* **94**, 197201 (2005).
- [11] T. Onimaru, K. T. Matsumoto, Y. F. Inoue, K. Umeo, Y. Saiga, Y. Matsushita, R. Tamura, K. Nishimoto, I. Ishii, T. Suzuki *et al.*, *J. Phys. Soc. Jpn.* **79**, 033704 (2010).
- [12] T. Onimaru, K. T. Matsumoto, Y. F. Inoue, K. Umeo, T. Sakakibara, Y. Karaki, M. Kubota, and T. Takabatake, *Phys. Rev. Lett.* **106**, 177001 (2011).
- [13] A. Sakai and S. Nakatsuji, *J. Phys. Soc. Jpn.* **80**, 063701 (2011).
- [14] K. Matsubayashi, T. Tanaka, A. Sakai, S. Nakatsuji, Y. Kubo, and Y. Uwatoko, *Phys. Rev. Lett.* **109**, 187004 (2012).
- [15] T. J. Sato, S. Ibuka, Y. Nambu, T. Yamazaki, T. Hong, A. Sakai, and S. Nakatsuji, *Phys. Rev. B* **86**, 184419 (2012).
- [16] M. Koseki, Y. Nakanishi, K. Deto, G. Koseki, R. Kashiwazaki, F. Shichinomiya, M. Nakamura, M. Yoshizawa, A. Sakai, and S. Nakatsuji, *J. Phys. Soc. Jpn.* **80**, SA049 (2011).
- [17] T. U. Ito, W. Higemoto, K. Ninomiya, H. Luetkens, C. Baines, A. Sakai, and S. Nakatsuji, *J. Phys. Soc. Jpn.* **80**, 113703 (2011).
- [18] M. Matsunami, M. Taguchi, A. Chainani, R. Eguchi, M. Oura, A. Sakai, S. Nakatsuji, and S. Shin, *Phys. Rev. B* **84**, 193101 (2011).
- [19] Y. Tokunaga, H. Sakai, S. Kambe, A. Sakai, S. Nakatsuji, and H. Harima, *Phys. Rev. B* **88**, 085124 (2013).
- [20] D. L. Cox, *Phys. Rev. Lett.* **59**, 1240 (1987).
- [21] A. Sakai, K. Kuga, and S. Nakatsuji, *J. Phys. Soc. Jpn.* **81**, 083702 (2012).
- [22] See Supplemental Material, which includes Refs. [23–29], at <http://link.aps.org/supplemental/10.1103/PhysRevLett.113.267001> for experimental details.
- [23] Y. Matsumoto *et al.* (unpublished).
- [24] A. Aharoni, *J. Appl. Phys.* **83**, 3432 (1998).
- [25] R. Bachmann, F. J. J. Disalvo, T. H. Geballe, R. L. Greene, R. E. Howard, C. N. King, H. C. Kirsch, K. N. Lee, R. E. Schwall, H. U. Thomas *et al.*, *Rev. Sci. Instrum.* **43**, 205 (1972).
- [26] J. P. Shepherd, *Rev. Sci. Instrum.* **56**, 273 (1985).
- [27] Y. Matsumoto *et al.* (unpublished).
- [28] Y. Verbovytsky, K. Latka, and K. Tomala, *J. Alloys Compd.* **442**, 334 (2007).
- [29] M. Koga and H. Shiba, *J. Phys. Soc. Jpn.* **66**, 1485 (1997).
- [30] R. A. Hein and R. L. Falge, *Phys. Rev.* **123**, 407 (1961).
- [31] N. R. Werthamer, E. Helfand, and P. C. Hohenberg, *Phys. Rev.* **147**, 295 (1966).
- [32] E. Helfand and N. R. Werthamer, *Phys. Rev.* **147**, 288 (1966).
- [33] M. Kubota, H. R. Folle, C. Buchal, R. M. Mueller, and F. Pobell, *Phys. Rev. Lett.* **45**, 1812 (1980).
- [34] K. Araki, Y. Shimura, N. Kase, T. Sakakibara, A. Sakai, and S. Nakatsuji, *JPS Conf. Proc.* **3**, 011093 (2014).
- [35] A. Sakai and S. Nakatsuji, *J. Korean Phys. Soc.* **63**, 398 (2013).
- [36] S. Ishihara, Y. Murakami, T. Inami, K. Ishii, J. Mizuki, K. Hirota, S. Maekawa, and Y. Endoh, *New J. Phys.* **7**, 119 (2005).